British Journal of Pharmaceutical and Medical Research Vol.03, Issue 06, Pg.1478 - 1493, November-December 2018

Available Online at http://www.bjpmr.org

BRITISH JOURNAL OF PHARMACEUTICAL AND MEDICAL RESEARCH

Cross Ref DOI : https://doi.org/10.24942/bjpmr.2018.390 Volume 03, Issue 06 Nov-December 2018

ISSN:2456-9836
ICV: 60.37

Research Article

Structure-Based Design Of Tripeptide Derivatives Of α - Aminoalkylphosphonate Esters For Prostate-Specific Antigen Inhibition

Arben Kojtari[1], Jacob Babinec[1], Vishal Shah[1], Catherine Yang[2], and Hai-Feng Ji[1]

[1]Department of Chemistry, Drexel University, Philadelphia, PA 19104

[2]Department of Basic Sciences, College of Medicine, California North state University, Elk Grove, CA 95757

ARTICLE INFO

Article History:
Received on 06th Nov, 2018
Peer Reviewed on 24th Nov, 2018
Revised on 11th December, 2018
Published on 28th December, 2018

Keywords:
Prostate-Specific Antigen, Autodock, Molecular Docking, Flexible Sidechain

ABSTRACT

Recently, we reported a new lead compound *R/S*-diphenyl[N-benzyloxycarbonylamino(4-carbamoylphenyl) methyl] phosphonate as an inhibitor of prostate-specific antigen (PSA), for the control of prostate tumor progression.[1] In this work, additional tripeptide derivatives of the lead compound were modeled using a similar approach. An incremental build method was utilized to improve computational efficiency of peptide docking. Molecular dynamics (MD) simulations were used to obtain trajectories of selected ligands and validate key interactions in the binding complexes. Additionally, the importance of the classic kallikrein loop (CKL) and its interaction with the extended substrate were highlighted in the MD analysis. This modeling study introduces tripeptide derivatives of aminoalkylphosphonates as stronger PSA inhibitors for prostate cancer treatment.

Corresponding Author: *Hai-Feng Ji, Department of Chemistry, Drexel University, Philadelphia, PA 19104.* hj56@drexel.edu

INTRODUCTION:

Prostate Specific Antigen (PSA) is an intriguing protease due to its implications in prostate cancer, where its role is often viewed as enigmatic. PSA is normally released from prostatic tissue into seminal fluid, where its primary role is limited to cleaving semenogelin I and II, which are responsible for gelation of semen.[2] However, PSA has been shown to leak into blood plasma, where it is normally not found or nearly absent, in the event of prostate cancer (PCa). Consequently, it is used as a biological indicator for the progression of the disease state.[3–5] Some evidence has shown that PSA is responsible for activating growth factors that are responsible for carcinogensis, although the results have been limited to *in vitro* studies.[6–8] Despite this, researchers continue to pursue the serine protease as a potential therapeutic target since inhibiting PSA could potentially block/reduce proliferation or metastasis of PCa cells.

PSA belongs to the human tissue kallikrein (KLK) class of proteins. The subgroup kallikrein contains serine proteases exclusively, with all KLK proteins containing the conserved catalytic triad of HIS_{57}, ASP_{102}, and SER_{195} that is responsible for their proteolytic activity.[9] The mechanism of catalysis requires SER_{195} acting as the nucleophile by attacking the carbonyl of the peptide bond with assistance from HIS_{57} (directly) and ASP_{102} (indirectly). A tetrahedral intermediate is formed, which is subsequently broken upon expulsion of the leaving group containing the NH_2-terminus, while the acyl-enzyme complex is produced. Deacylation is facilitated by a hydrolytic water molecule, forming a second tetrahedral intermediate. This intermediate collapses, producing the carboxylic acid and restoring SER_{195} in the process. This truncated enzymatic mechanism is shown schematically in **Figure 1**.[9]

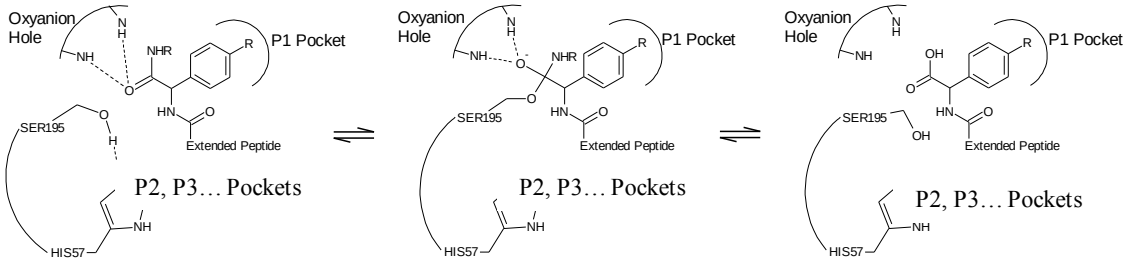

Figure 1 – Peptide substrate binding mechanisms with serine proteases, showing cleavage at the COOH-terminus of the phenylglycine residue. Binding of peptide substrate, formation of tetrahedral intermediate, and subsequent amide scission.

Aside from the catalytic triad, binding "grooves" or "pockets" within the active site are also present and play an important role in substrate recognition. These discrete pockets, denoted as P1, P2, P3, etc., vary in their chemical environments depending on kallikrein type. The substrate for serine proteases are peptides, where substrate recognition is determined by the amino acid side-chain. The amino acid of the peptide substrate that has affinity for the P1 pocket is termed S1, P2 pocket affinity is termed S2, and so on.

Serine proteases have been previously targeted for therapeutic purposes. For example, thrombin, which is responsible for coagulation and clotting in the blood via activation of platelets,[10] is targeted using peptides and their analogues as inhibitors. A receptor inhibitor is a molecule that blocks or reduces a protein's function. Thrombin is targeted using inhibitors in the event of deep vein thrombosis, where there is significant blood clotting within the deep system. A portion of the clot can break off and travel to the lungs or brain, causing a pulmonary embolism or stroke. Tryptase, a trypsin-like serine protease, has also been targeted for its therapeutic potential. Tryptase, which are secreted outside of mast cells within dense granules, play a pro-inflammatory role in the lungs. The response, typically in the presence of an allergen, causes inflammation and is directly linked to asthma and allergic disorders.

Some PSA inhibitors have been developed.[11-13] However, these inhibitors only display moderate efficacy as PSA inhibitors. Recently, we reported a new lead compound **1** (diphenyl[N-benzyloxycarbonylamino(4-carbamoylphenyl)methyl]phosphonate, **Figure 2**) as a PSA inhibitor. The α-aminoalkylphosphonates have previously shown inhibition of a variety of serine proteases[9,14-16] and can be tuned synthetically to be site-specific for the P1 pocket of the protein. It was determined by the docking studies that **1** had scored the highest out of chosen compounds in our study, with a free energy score of -8.29/-9.14 kJ·mol^{-1} for *R/S*, respectively. Experimental data showed the IC50 of this compound is 0.25 □M. The model predicts that both hydroxyls of THR_{190} and SER_{227} form hydrogen bonds with the C=O of the carbamoyl. Concurrently, the amide proton forms a hydrogen bond within the distance of 2.2 Å of the carbonyl of the SER_{217} amide.

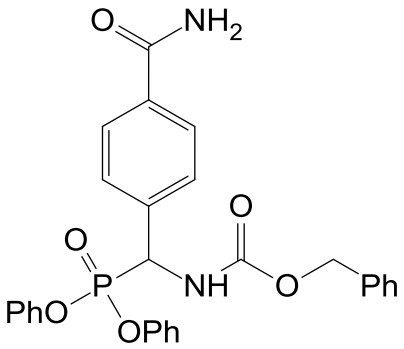

Figure 2. Structure of compound 1

In this work, we continue to use the structure-based drug design to perform molecular docking in order to further optimize the molecular structures for high binding scores. Peptide derivatives of the S1-substrate were modeled according to virtual screening results of 722 tripeptide mimics (19x19 amino acids, each include S and R isomers on P, both *R*- and *S*-enantiomers of **1**, were used for the simulations to elucidate any differences between the two binding events.) using an incremental grow method using the AutoDock suite. Ligand docking experiments of tripeptide mimics containing the S1 phenylglycine derivative (**Figure 3**) were performed using an approach similar to anchor-and-grow/ incremental build methodologies.[17] To achieve this, the binding pose generated for compound **1** was used as the rigid anchor. Naming of atoms with associated amino acid fragments of the ligand are shown in **Figure 3**. The benzyloxycarbonyl (also called Carboxybenzyl, Cbz) group was removed from the structure and S2 & S3 amino acids were added to the N-terminus of the S1 anchor. All geometry optimizations were performed using the Dreiding force field. The .pdbqt ligand files were prepared using the ADT 1.5.6 GUI to restrict bond torsions of the anchor, thereby reducing the pose space searched for the ligand and limited to only the dipeptide torsions for consideration in the global search. In addition, the rigid anchor preserves the binding pose associated with the phenylglycine residue and retains pairwise interactions between S1 and P1 groups. In total, 722 ligands were compiled and screened using the Raccoon AutoDock Virtual Screen.[18] Combinations of 19 primary D-amino acids were used.

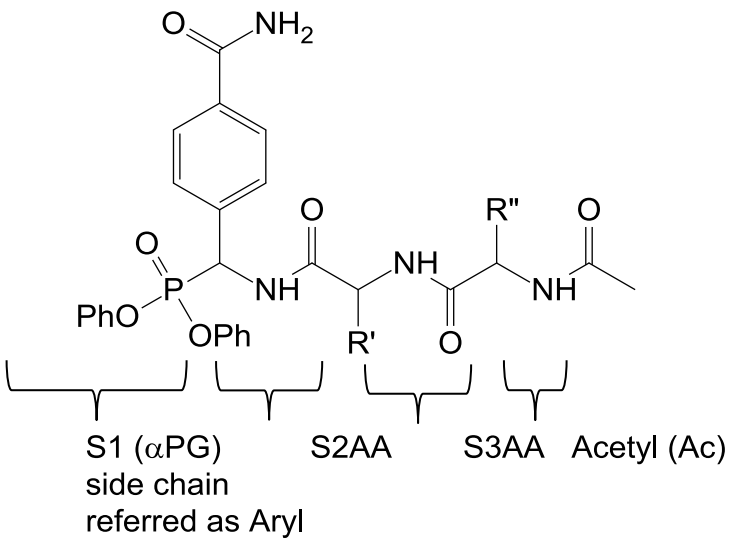

Figure 3– Atom/group assignments of the tripeptide mimics containing the S1 phenylglycine derivative.

2. Results and discussion.

2. 1. AutoDock Optimization

In order to determine the ligand poses of tripeptide substrates and calculate binding energies efficiently, a pseudo-incremental build approach was developed. The rationale behind this was that earlier experiments using a very flexible tripeptide ligand resulted in an incomplete minimization process due to the number of rotatable bonds typically exceeding 15 torsions. Because of the large sampling necessary for the pose space, the S1 fragment of the ligand was treated as a rigid anchor by restricting sampled torsional degrees of freedom. S1 fragment poses were constructed from CTC docking studies described previously in this chapter. Using LGA search optimization with random seeding, the S1 fragment is docked into the P1 site far more consistently than using a non-rigid anchor.

The assumption being made in incremental build models is that the binding pose of the fragment(s) are identical or similar to the composite of the fragments. In regards to the tripeptide mimics described here, we assume that the S1 fragment is exclusive to the P1 site, but the S2 and S3 fragments do not necessarily have to be exclusive to the respective P2 and P3 pockets. As a consequence, the S2S3 dipeptide was treated as a single, flexible fragment. This approach was successful in providing ligand poses with appropriate docking energies. An alternate method would have been to build every amino acid fragment incrementally to reduce the torsional degrees of freedom. However, although systematically sampling and building each amino acid fragment would be time-consuming, it is a very feasible option if necessary for the molecular docking problem.

Of the 722 tripeptide ligands sampled using global optimization, all fragments sampled for the S2 and S3 positions contained the D-isomer of the corresponding amino acids (AA), D-amino acids are not subject to proteolytic cleavage from PSA and other endogenous proteases. Results from the molecular docking studies of the tripeptide mimics can be found in the supporting information, top scoring poses are summarized in **Table 1**. From the docking studies, peptides containing a Trp, Phe or Tyr at the S2 position correlated to higher docking scores. The P2 site appears to accommodate larger side chains, such as ring structures, in the hydrophobic pocket. For the S3 site, Gly, Ala, and Pro residues are associated with higher scoring ligand poses. The P3 pocket is significantly smaller in solvent-accessible surface area when compared to the P1 and P2 sites. Not surprisingly, only smaller side chain residues can fit into the site, which is located in the CKL channel extending out towards the outer surface of the protein.

Table 1 – Selected AutoDock binding scores of tripeptide diphenyl phosphonates.

S3 D-AA	S2 D-AA	Binding Score (kJ/mol)
Val	Leu	R: -8.00 S: -12.25
His	Ile	R: -7.63 S: -11.65
Pro	Trp	R: -11.13 S: -9.75
Pro	Tyr	R: -10.08 S: -11.40
Tyr	Val	R: -9.48 S: -11.31
Ala	Trp	R: -10.32 S: -10.20
Ala	Tyr	R: -10.36 S: -9.63
Gly	Phe	R: -11.17 S: -10.30
Met	Trp	R: -11.07 S: -10.67
Trp	Ala	R: -6.62 S: -11.30
Gly	Trp	R: -10.47 S: -10.85
Lys	Gly	R: -11.29 S: -5.99

The results show some semblance to work previously published by G.S. Coombs *et al*.[19] Using substrate phage display, the authors were able to elucidate optimal substrate profile via consensus. From their results, P1 was specific for Tyr residues, P2 also displayed Tyr preference (although residues Ala, Arg, Gly, Leu, Phe, Ser, and Val evidenced similar partiality), and P3 preferred Ser (in addition to Ala, Arg, and Thr).[19] More recent research performed by LeBeau et al. showed pocket specificity of Leu and Lys at the S2 and S3 positions, respectively, but Tyr can also be substituted with Leu at the S1 site.[20] Other studies also reported varied substrate preference for S2 and S3, including Gln for both sites on the peptide substrate.[21] From literature on PSA hydrolysis of peptide or peptidomimetic substrates, there is no clear consensus for amino acid preference occupying the S2 & S3 positions. Similar to the docking results detailed here, broad trends are apparent but there is not an absolute solution to determining the optimal side chain fragment.

There are obvious exceptions to the aforementioned P2 & P3 pocket and trends for substrate preference in the molecular docking studies. The ligand Ac-Gly-D-Trp-(4-$CONH_2$PhGly)$^P(OPh)_2$ binding pose displayed the S2-Trp side chain angled through the peptide groove towards the P3 site and the S3-Gly towards the P2 site **(Figure 4)**. Ligands Ac-D-His-D-Ile-(4-$CONH_2$PhGly)$^P(OPh)_2$ and Ac-D-Pro-D-Tyr-(4-$CONH_2$PhGly)$^P(OPh)_2$ showed similar top scoring substrate poses in the PSA binding site. The top scoring pose sampled, Ac-D-Val-D-Leu-(4-$CONH_2$PhGly)$^P(OPh)_2$, contained hydrophobic side chains where one diastereomer scored significantly

higher compared to its stereoisomer. The docking obtained for the *S*-chirality at the α-phenylglycine (αPG) anchor is -12.25 kJ·mol^{-1} and side chain placements of the extended substrate located within expected pocket sites. The ligand Ac-Gly-D-Phe-(4-$CONH_2$PhGly)$^P(OPh)_2$ also conserved proper side chain placements for both diastereomers (-11.17 & -10.30 kJ·mol^{-1} for *R/S*-αPG) Although the *R*-αPG anchor scored lower than its diastereomer, this was found not to be a consistent trend within the data set. Rather, top scoring poses obtained from the VS appear to be more random rather than a shared trend between diastereomers (**Figure 5**).

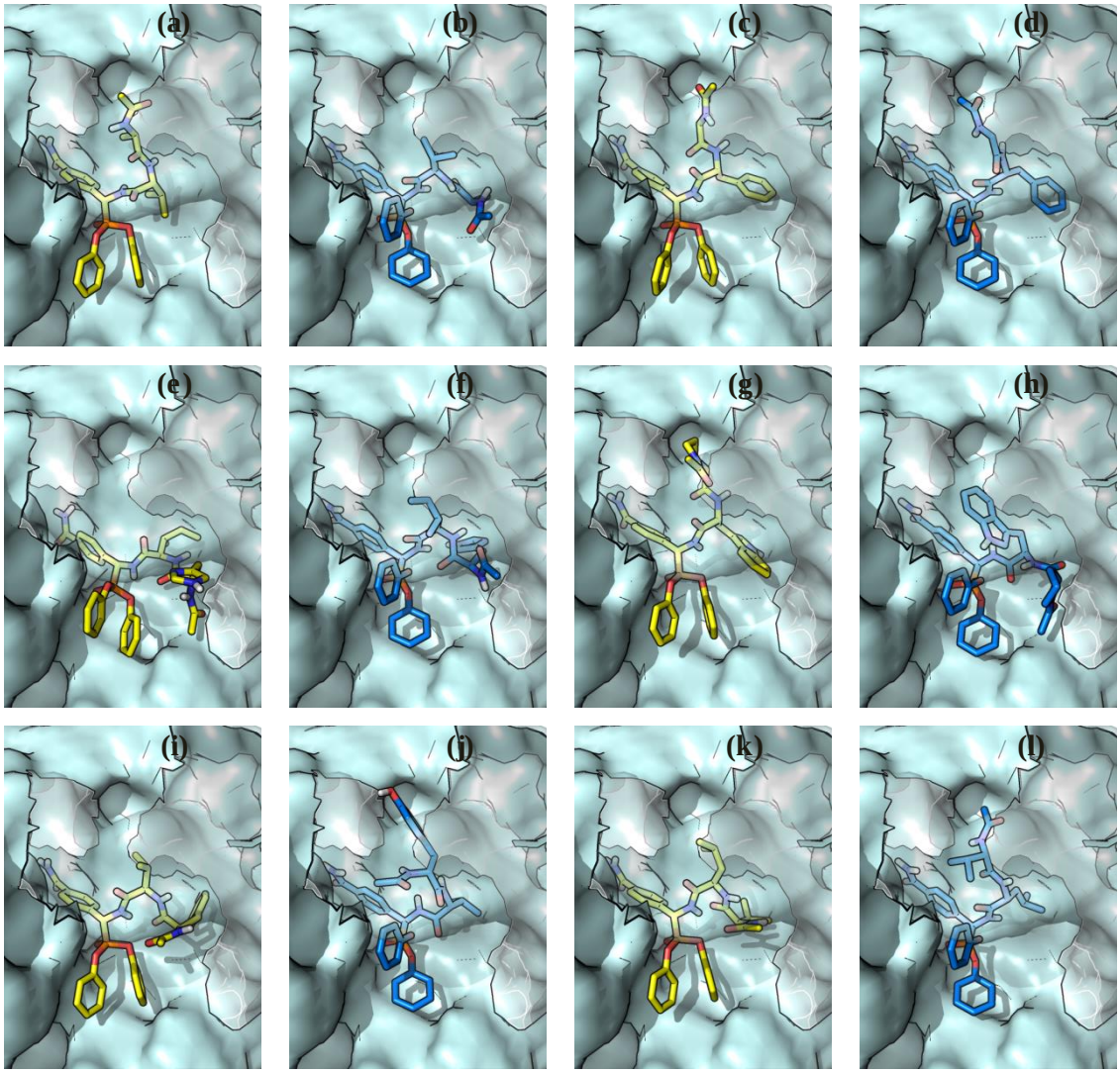

Figure 4 – (a&b) Ac-Ala-Val (c&d) Ac-Gly-Phe-(e&f) Ac-His-Il- (g&h) Ac-Pro-Trp (i&j) Ac-Tyr-Val (k&l) Ac-Val-Leu. R-αPG anchors are in yellow, S-αPG anchors are in blue. CKL is displayed with 50% transparency to visualized peptide binding groove.

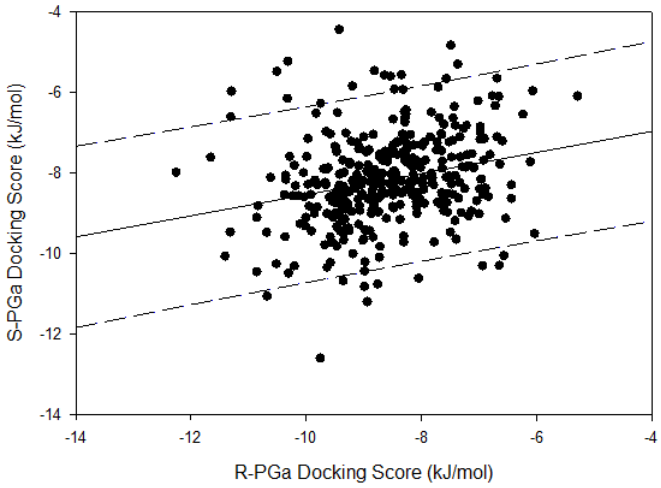

Figure 5– Scatterplot of peptidomimetic ligands comparing R- and S-αPG anchors and the shared extended substrate peptide fragments.

2.2. Molecular dynamics (MD) simulations

MD simulations were performed using GROMACS version 4.6.5[22] with the similar method in our previous study.[1] Select peptidomimetic substrates were also chosen for MD studies using their minimized docking pose obtained from AutoDock. The PSA crystal structure was modified similar to that reported in the molecular docking studies in our previous study. In addition, the two sugar moieties from the PSA crystal structure file were removed for the MD simulations to facilitate topology assignments.

A visual representation of the equilibrated protein-solvent system is shown in **Figure 6**. The pertaining plots used in the simulation were created with the GROMACS v4.6.5 package. Xmgrace GUI used to visualize them accordingly. A Perl script was used to visually represent the hydrogen bond prevalence between ligand and protein atoms, exclusively. Donor-acceptor distances were restricted to 3.5 Å with an angle cutoff of 30º. To analyze amide backbone geometries in both static and dynamic models, Bendix 1.1 was used as a VMD plugin to generate contour plot data of angle vs. time per residue.[23]

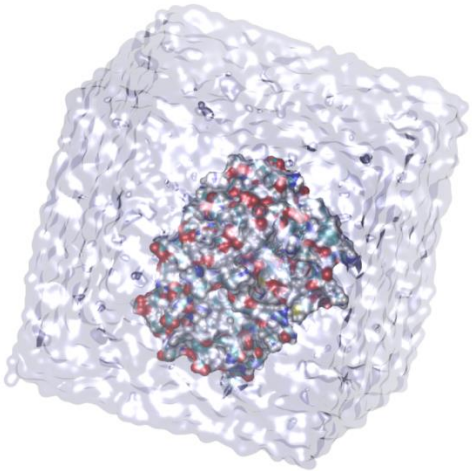

Figure 6 –MD representation of PSA in a solvated cube.

A control simulation was performed with PSA alone in a solvated cube to compare B-factors from the crystallographic structure to those calculated from the MD simulation.[24] Compound **1** was initially modeled dynamically to test its overall binding stability, deviations of protein structure, fluctuations of local residues, and the retention of ligand hydrogen bond contacts. Good qualitative agreement was achieved, allowing further simulations to be conducted with similar parameters already established from this control experiment.[1] B-factors indicate thermal motion paths for the ligand in the binding event, giving credence that larger substrate preferentially extend through the binding groove of PSA rather than outward towards bulk solvent.

2.2a Ac-D-Val-D-Leu-(4-CONH$_2$-PhGly)^P(OPh)$_2$

The binding complex of the peptidomimetic substrate of Ac-D-Val-D-Leu-(4-CONH$_2$-PhGly)^P(OPh)$_2$ within the PSA active site was modeled using MD to assess ligand and protein trajectories. The tripeptide ligand was the top scored ligand from the AutoDock VS of 722 peptide-like substrates, a major contributing factor to the ligand choice for the MD simulation.

RMSD analysis of the ligand and PSA is shown in **Figure 7**. During the 5 ns MD simulation, the RMSD for both bodies were recorded less than 0.20 nm, with the ligand fluctuating steadily at approximately 0.15 nm. The trajectories of the binding complex stabilizes after 2 ns of the simulation and the calculated RMSD hits a plateau thereafter. This is indicative of stabilization of the binding complex in the simulation, retaining the majority of the input coordinates of the ligand without significant deviation and thus giving credence to the minimized pose obtained from AutoDock.

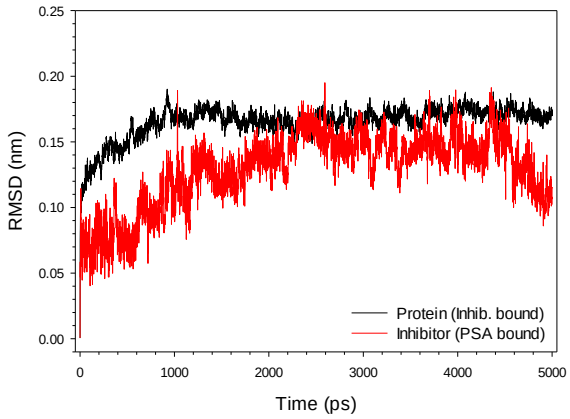

Figure 7 – RMSD plot of the inhibitor Ac-D-Val-D-Leu-(4-CONH$_2$-PhGly)^P(OPh)$_2$ & protein in the binding complex.

RMSF plots and B-factor representation of the binding complex is agreeable with the expectations of the binding complex stabilization mechanism. The marked decrease in CKL fluctuation is directly coupled to the ligand binding event, which can be deduced when comparing to the solvated protein, alone (**Figure**). All but one CKL residue, ARG$_{95J}$, has an RMSF less than 0.20 nm during the simulation. The reason behind this decrease in CKL RMSF can be attributed to non-bonded interactions. Looking at the hydrogen-bonding map, ARG$_{95G}$ and LEU$_{95I}$ of the CKL play integral roles in stabilizing ligand trajectory in the binding site. ARG$_{95G}$ guanidino protons form hydrogen bonds with ^{Leu}C**O**NH of the peptide substrate, while the amide proton of LEU$_{95I}$ stabilize the N-acetyl protecting group of the ligand via hydrogen bonding with ^{Ac}C**O**. The total mapped incidences of hydrogen bonding for the aforementioned interaction pairs are ~67% and 94.9%, respectively.

(a) **(b)**

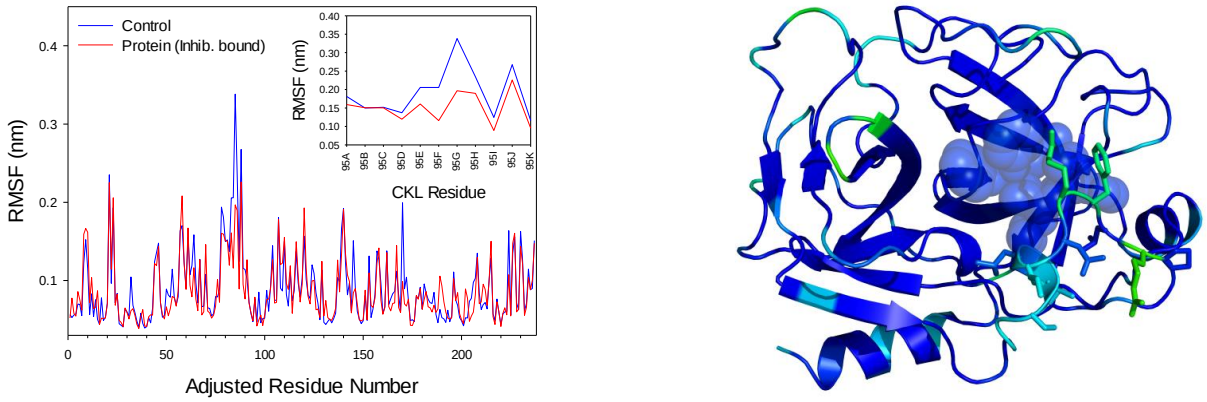

Figure 8 - (a) RMSF of the 237 residues of PSA with the CKL residues shown in the inset. (b) B-factor representation of the protein with Ac-D-Val-D-Leu-(4-CONH$_2$PhGly)^P(OPh)$_2$ bound. Color scale: >0.30 nm – red; >0.25 nm – yellow; >0.20 nm – green; >0.15 nm – cyan; <0.15 nm – blue. CKL side chains are displayed only. Ligand is represented as blue spheres.

Additionally, the ligand fragment Val-Leu amide groups act as proton donors with residues GLY_{216} and ARG_{95G}. The prevalence of these hydrogen bonding contacts are shown in Table 2. The carbonyls of the PSA residues form a very stable hydrogen bonding network with the ligand backbone with a significant degree of incidence (88.3% and 98.1% for GLY_{216} and ARG_{95G}, respectively). Moreover, the GLY_{216} amide proton was observed to hydrogen bond with ^{Val}CONH, although the frequency of this interaction was less than 5% in occurrence. More importantly, these interactions are expected for peptide-like substrates, especially with residues 216-218 located across from the CKL.[19] Interactions with key P1 residues of THR_{190}, SER_{217}, and SER_{227} were similar to those highlighted in PSA-**S-1** complex MD simulation, although polar contact incidence between SER_{217} and the substrate was significantly reduced.

Table 2 – Hydrogen bond prevalence map of PSA interactions with Ac-D-Val-D-Leu-(4-CONH$_2$-PhGly)^P(OPh)$_2$ inhibitor. Interacting atom pairs are in bold.

H-Donor	Donor Atom	H-Acceptor	Acceptor Atom	% Existence
Ligand	^{Val}CON**H**	GLY_{216}	C**O**NH	88.322
Ligand	^{Leu}CON**H**	ARG_{95G}	C**O**NH	98.080
Ligand	$^{\alpha PG}$CON**H**	SER_{214}	C**O**NH	1.820
Ligand	^{Aryl}CON**H**$_2$	THR_{190}	**O**H	17.317
Ligand	^{Aryl}CON**H**$_2$	THR_{190}	C**O**NH	12.018
Ligand	^{Aryl}CON**H**$_2$	SER_{217}	C**O**NH	4.019
Ligand	^{Aryl}CON**H**$_2$	SER_{227}	**O**H	7.618
ARG_{95G}	N**H**C(NH$_2$)$_2^+$	Ligand	^{Leu}C**O**NH	19.276
ARG_{95G}	N**H**C(NH$_2$)$_2^+$	Ligand	PO(**O**Ph)	31.714
ARG_{95G}	N**H**C(NH$_2$)$_2^+$	Ligand	PO(**O**Ph)	1.340
ARG_{95G}	NHC(N**H**$_2$)$_2^+$	Ligand	^{Leu}C**O**NH	47.570
LEU_{95I}	CON**H**	Ligand	^{Ac}C**O**	94.921

THR_{190}	O**H**	Ligand	^{Aryl}C**O**NH_2	62.947
GLY_{193}	CON**H**	Ligand	P**O**(OPh)	85.483
SER_{195}	O**H**	Ligand	PO(**O**Ph)	1.840
GLY_{216}	CON**H**	Ligand	^{Val}C**O**NH	4.639
SER_{227}	O**H**	Ligand	^{Aryl}C**O**NH_2	14.897

Further analysis of the MD simulation reveals conservation of appropriate S/P placements within the active site. S2-Leu side chain remains exclusively in the P2 site while the S3-Val extends through the peptide-binding groove. The S2-Leu is flanked by LEU_{95C} and LEU_{95I} side chains to accommodate the hydrophobic fragment (**Figure**), which has been reported before in crystallographic studies.[25] Surprisingly, the bulky S3-Val side chain does not deviate significantly during the simulation. Although the side chain is not found to be directly in the small P3 site, its coordinates were retained in the groove region of PSA

.

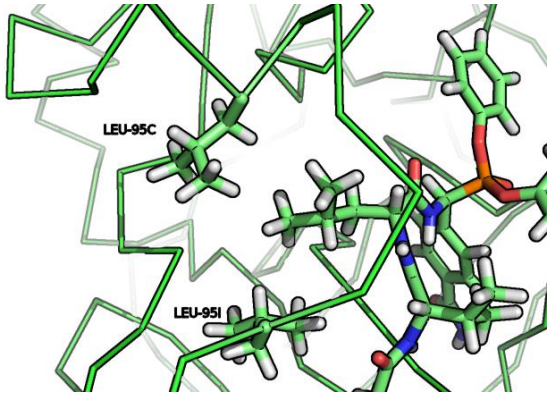

Figure 9 – P2 site residues LEU_{95C} and LEU_{95I} flanking the S2 residue of compound Ac-D-Val-D-Leu-(4-$CONH_2$PhGly)^P(OPh)$_2$.

2.2b. Ac-Gly-D-Phe-(4-$CONH_2$-PhGly)^P(OPh)$_2$

MD simulation of this tripeptide mimic provided some exceptional results compared to other modeled ligands. From molecular docking studies, the ligand displayed very modest docking scores for the diastereomers. Trajectories of the binding complex was mapped and the dynamic RMSD was recorded (**Figure**). The ligand stabilizes shortly after the initiation of the simulation, the fastest to relax out of all MD simulations performed. RMSD of the ligand and the receptor remains at approximately 0.15 nm for the majority of the 5 ns run, evidence of a binding complex that was optimized close to the global minimum in the docking studies.

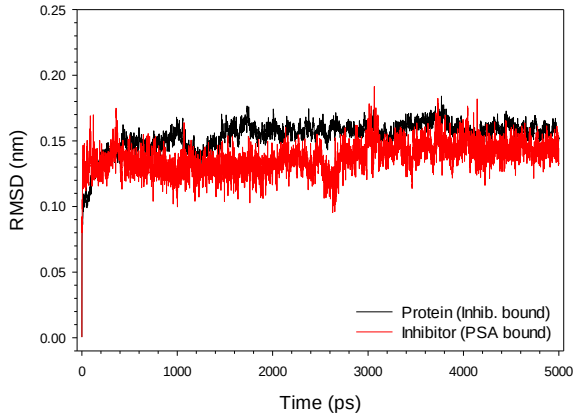

Figure 10 – RMSD plot of the inhibitor Ac-Gly-D-Phe-(4-CONH$_2$-PhGly)^P(OPh)$_2$ & protein in the binding complex.

RMSF analysis reveals a reduction of CKL residue fluctuations throughout the simulation (**Figure 11**). Compared to the control trajectory file, CKL deviations are mostly reduced to below 0.15 nm, including solvent accessible residues of LYS$_{95E}$, ASN$_{95F}$, ARG$_{95G}$, PHE$_{95H}$, and ARG$_{95J}$. LEU$_{95D}$ and LEU$_{95I}$ were the exceptions to the overall trend, with RMSF observed to be above 0.15 nm and greater than fluctuations in the control simulation. These CKL fluctuations can be further explained by examining dynamic polar interactions within the simulation.

(a) **(b)**

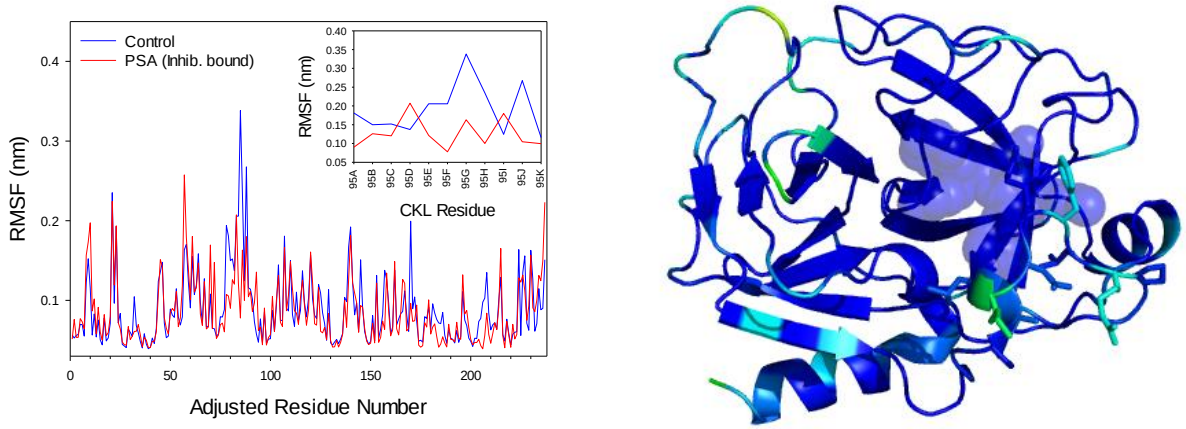

Figure 11 - (a) RMSF of the 237 residues of PSA with the CKL residues shown in the inset. (b) B-factor representation of the protein with Ac-Gly-D-Phe-(4-CONH$_2$PhGly)^P(OPh)$_2$ bound. Color scale: >0.30 nm – red; >0.25 nm – yellow; >0.20 nm – green; >0.15 nm – cyan; <0.15 nm – blue. CKL side chains are displayed only. Ligand is represented as blue spheres.

The hydrogen bond map for this tripeptide is quite unique when compared to other modeled ligands (**Table 3**). As expected, key S1 interactions were conserved between P1 residues of THR$_{190}$ (O**H**), SER$_{217}$ (C**O**NH), and SER$_{227}$ (O**H**) between the carbamoyl functionality of the ligand and with retained hydrogen bonding for the duration of the 5 ns simulation. Interactions are prevalent for more than

93.0%, 91.4% and 82.1% for the trio of residues 190, 217, and 227, respectively, and facilitate locking of the peptide to the protein.

In conjunction with S1/P1 interactions, S2 and S3 amide backbone hydrogen bonding play an important role in the stability of the bound ligand. GLY_{216} and GLU_{218} amide protons hydrogen bond with the ligand's $^{Gly}C\mathbf{O}NH$ and $^{Ac}C\mathbf{O}$ carbonyls with a prevalence of 93% and 62 %, respectively. In addition, the ARG_{95G} guanidine group interacts with $^{Phe}C\mathbf{O}NH$ carbonyl with greater than 70.4% incidence coupled with GLY_{193} stabilizing the oxyanion hole with the phosphonate moiety (87.1% prevalence) to form an amide back bone zipper between S1-S3 amino acids and PSA. Similar hydrogen bonding interactions were highlighted in a PSA crystallography study published by Ménez *et al*. in 2008, where the authors described the formation of a short anti-parallel β-zipper between a co-crystallized peptide substrate and PSA.[25] The preponderance of the four residues forming backbone interactions in the trajectory files appear to highlight the stability of the complex, especially evident when comparing the interaction maps to ligand RMSD. Although S2 & S3 amino acid side chains cannot interact via intermolecular hydrogen bonding with P2 & P3 residues, the size of each side chain appears to accommodate the pockets well enough to help stabilize the binding complex.

Table- Hydrogen bond prevalence map of PSA interactions with Ac-Gly-D-Phe-(4-$CONH_2$-PhGly)$^P(OPh)_2$ inhibitor. Interacting atom pairs are in bold.

H-Donor	Donor Atom	H-Acceptor	Acceptor Atom	% Existence
Ligand	$^{Gly}CON\mathbf{H}$	GLU_{218}	$CO\mathbf{O}^-$	5.299
Ligand	$^{Gly}CON\mathbf{H}$	GLU_{218}	$CO\mathbf{O}^-$	5.559
Ligand	$^{Aryl}CON\mathbf{H}_2$	THR_{190}	$C\mathbf{O}NH$	4.499
Ligand	$^{Aryl}CON\mathbf{H}_2$	SER_{217}	$C\mathbf{O}NH$	91.362
Ligand	$^{Aryl}CON\mathbf{H}_2$	SER_{227}	$\mathbf{O}H$	2.340
ARG_{95G}	$NHC(N\mathbf{H}_2)_2^+$	Ligand	$^{Phe}C\mathbf{O}NH$	70.446
THR_{190}	$O\mathbf{H}$	Ligand	$^{Aryl}C\mathbf{O}NH_2$	93.141
GLY_{193}	$CON\mathbf{H}$	Ligand	$P\mathbf{O}(OPh)$	87.143
SER_{195}	$O\mathbf{H}$	Ligand	$P\mathbf{O}(OPh)$	1.680
GLY_{216}	$CON\mathbf{H}$	Ligand	$^{Gly}C\mathbf{O}NH$	93.041
GLU_{218}	$CON\mathbf{H}$	Ligand	$^{Ac}C\mathbf{O}$	62.088
SER_{227}	$O\mathbf{H}$	Ligand	$^{Aryl}C\mathbf{O}NH_2$	82.064

2.2c. Ac-Gly-D-Trp-(4-$CONH_2$-PhGly)$^P(OPh)_2$

A simulation of a ligand containing Trp at S2 and Gly at S3 was performed to probe the dynamics of the binding complex (**Figure 12**). The peptidomimetic is unique compared to others modeled, one reason being the abundance of Trp-containing ligands with modest docking scores in the VS. As mentioned before, it is somewhat suprising since no other peptide substrates for PSA has shown Trp preference at the S2 position. From RMSD analysis, the binding complex is in flux until after 3500 ps, at which is it considered to have "relaxed." Prior to the conformational shift event, the ligand fluctuates from 0.15 nm and descends to 0.10 nm, then abruptly jumps to over 0.20 nm. At the same instance, no major deviations in the protein structure is observed.

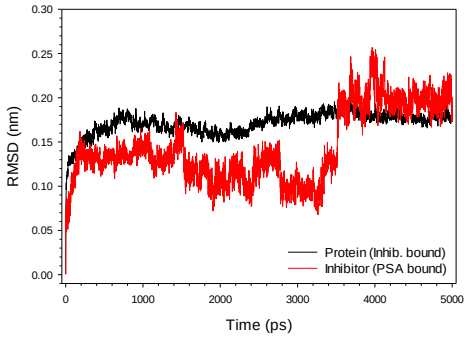

Figure 12 – RMSD plot of the inhibitor Ac-Gly-D-Trp-(4-CONH$_2$-PhGly)^P(OPh)$_2$ & protein in the binding complex.

RMSF plots of PSA residues display substantial fluctuations of CKL residues compared to other peptidomimetic compounds. Aside from ARG$_{95G}$, CKL side chain deviations were similar to that of the control MD run (**Figure 13**). This is indicative of one or more possibilities; that the ligand is a poor binder to the PSA active site due to complex "wiggling" or the input docking pose is not properly optimized. It is believed that the latter is more likely responsible for the former observation since S2S3-P2P3 interacting domains are not conserved. This rationale is supported by the interaction maps provided (**Table 4**).

(a) **(b)**

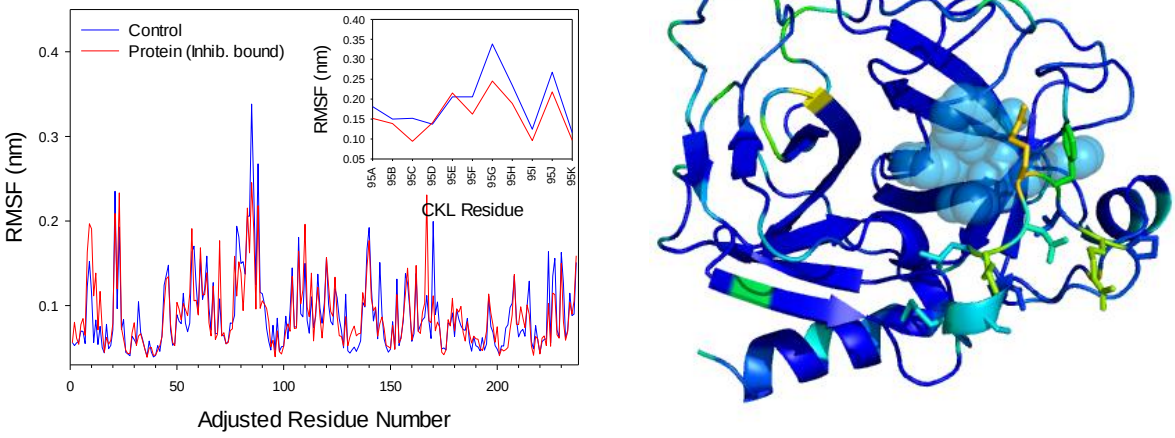

Figure 13 - (a) RMSF of the 237 residues of PSA with the CKL residues shown in the inset. B-factor representation of the protein with Ac-Gly-D-Trp-(4-CONH$_2$PhGly)^P(OPh)$_2$ bound. Color scale: >0.30 nm – red; >0.25 nm – yellow; >0.20 nm – green; >0.15 nm – cyan; <0.15 nm – blue. CKL side chains are displayed only. Ligand is represented as blue spheres.

In the hydrogen bond prevalence map, the extended substrate lacks the stabilizing interactions as seen in other peptidomimetic compounds. ARG$_{95G}$ interactions are reduced significantly to less than 10% for key interactions with substrate amide backbone. Aside from P1 residue triad and P=O stabilization by GLY$_{193}$, interactions are limited and insignificant in terms of hydrogen bonding. THR$_{190}$, SER$_{217}$, and SER$_{227}$ interactions were within expectations for % occurance (total existence of 82.3%, 57.1% and 70.2%, respectively). From this, it can be predicted that the primary reason for substrate binding to PSA is dependent on S1/P1 interactions.

Table 4 - Hydrogen bond prevalence map of PSA interactions with Ac-Gly-D-Trp-(4-$CONH_2$-PhGly)$^P(OPh)_2$ inhibitor. Interacting atom pairs are in bold.

H-Donor	Donor Atom	H-Acceptor	Acceptor Atom	% Existence
Ligand	^{Gly}CON**H**	ASN_{95F}	C**O**NH	1.800
Ligand	^{Trp}CON**H**	LEU_{95C}	C**O**NH	5.239
Ligand	^{Aryl}CON**H**$_2$	THR_{190}	C**O**NH	6.279
Ligand	^{Aryl}CON**H**$_2$	SER_{217}	C**O**NH	57.129
ARG_{60}	NHC(N**H**$_2$)$_2^+$	Ligand	^{Ac}C**O**	8.358
ARG_{95G}	NHC(N**H**$_2$)$_2^+$	Ligand	^{Trp}C**O**NH	7.698
ARG_{95G}	NHC(N**H**$_2$)$_2^+$	Ligand	P**O**(OPh)	3.019
LEU_{95I}	CON**H**	Ligand	^{Trp}Indole-N**H**	5.059
THR_{190}	O**H**	Ligand	^{Aryl}C**O**NH$_2$	76.005
GLY_{193}	CON**H**	Ligand	P**O**(OPh)	64.207
GLY_{193}	CON**H**	Ligand	PO(**O**Ph)	14.497
SER_{227}	O**H**	Ligand	^{Aryl}C**O**NH$_2$	70.186

CONCLUSION

Docking of larger peptidomimetic ligands was achieved using a pseudo-incremental build model using a rigid phenylglycine fragment and a flexible anchor-bound dipeptide. The methodology employed was able to identify top hits for a tripeptide mimic from a modest library of 722 variants in the virtual screening. S1/P1 exclusivity was preserved, although not all S2/P2 & S3/P3 interacting domains followed the same pattern. The method is viable as a method for docking larger peptide-like compounds that contain an excessive number of torsions that may exceed the limits of the search function. Peptides are notorious in difficulty for molecular docking and the incremental build model is a suitable approach in docking large molecules.

From the MD studies, convergence of a stable binding complex within a solvated system is reached within the 5 ns simulation. Complex stability differences observed between peptidomimetic compounds were noticed, likely a product of the docking studies. In the example Ac-Gly-D-Trp-(4-$CONH_2$PhGly)$^P(OPh)_2$ where S2S3 and P2P3 interacting domains were not conserved, the ligand is shown to be in flux throughout most of the simulation time. The anchor-and-grow method described in the molecular docking study may need to be tuned to conserve these cross interactions, which appear to play a critical role in ligand stability. In conjunction with this, amide backbone stability facilitated by CKL residues and residues 216-218 is also imperative to binding. Furthermore, this relationship is reciprocated with reduced CKL fluctuations and stabilized angle distortions upon local conformational changes.

REFERENCE:

(1) Kojtari, A.; Shah, V.; Yang, C.; Ji, H.-F. "Structure-Based Design of Diphenyl - Aminoalkylphosphonates as Prostate-Specific Antigen Antagonists", J. Chem. Inform. Model. 2014, 54, 2967-2979.

(2) Lilja, H.; Oldbring, J.; Rannevik, G.; Laurell, C. B. " Seminal vesicle-secreted proteins and their reactions during gelation and liquefaction of human semen" J. Clin. Invest. 1987, 80, 281–285.

(3) Catalona, W. J.; Smith, D. S.; Ratliff, T. L.; Dodds, K. M.; Coplen, D. E.; Yuan, J. J.; Petros, J. A.; Andriole, G. L. " Measurement of Prostate-Specific Antigen in Serum as a Screening Test for Prostate Cancer" N. Engl. J. Med. 1991, 324, 1156–1161.

(4) Labrie, F.; Dupont, A.; Suburu, R.; Cusan, L.; Tremblay, M.; Gomez, J. L.; Emond, J. "Serum

Prostate Specific Antigen as Pre-Screening Test for Prostate Cancer" J. Urol. 1992, 147, 846–851.

(5) Stamey, T. A.; Yang, N.; Hay, A. R.; McNeal, J. E.; Freiha, F. S.; Redwine, E. "Prostate-specific antigen as a serum marker for adenocarcinoma of the prostate" N. Engl. J. Med. 1987, 317, 909–916.

(6) Balk, S. P.; Ko, Y. J.; Bubley, G. J. "Biology of prostate-specific antigen" J. Clin. Oncol. 2003, 21, 383–391.

(7) Crawford, E. D.; DeAntoni, E. P.; Ross, C. A. " The role of prostate-specific antigen in the chemoprevention of prostate cancer" J. Cell. Biochem. Suppl. 1996, 25, 149–155.

(8) Diamandis, E. P. "Prostate-specific antigen: a cancer fighter and a valuable messenger?" Clin. Chem. 2000, 46, 896–900.

(9) Oleksyszyn, J.; Boduszek, B.; Kam, C. M.; Powers, J. C. " Novel amidine-containing peptidyl phosphonates as irreversible inhibitors for blood coagulation and related serine proteases" J. Med. Chem. 1994, 37, 226–231.

(10) Davie, E. W.; Fujikawa, K.; Kisiel, W. " The coagulation cascade: initiation, maintenance, and regulation" Biochemistry 1991, 30, 10363–10370.

(11) Yang, C. F.; Porter, E. S.; Boths, J.; Kanyi, D.; Hsieh, M.-C.; Cooperman, B. S. " Design of synthetic hexapeptide substrates for prostate-specific antigen using single-position minilibraries" J. Pept. Res. 1999, 54, 444–448.

(12) LeBeau, A. M.; Singh, P.; Isaacs, J. T.; Denmeade, S. R. " Potent and Selective Peptidyl Boronic Acid Inhibitors of the Serine Protease Prostate-Specific Antigen"Chem. Biol. 2008, 15, 665–674.

(13) Singh, P.; Williams, S. A.; Shah, M. H.; Lectka, T.; Pritchard, G. J.; Isaacs, J. T.; Denmeade, S. R. " Mechanistic insights into the inhibition of prostate specific antigen by beta-lactam class compounds" Proteins 2008, 70, 1416–1428.

(14) Joossens, J.; Van der Veken, P.; Surpateanu, G.; Lambeir, A.-M.; El-Sayed, I.; Ali, O. M.; Augustyns, K.; Haemers, A. " Diphenyl Phosphonate Inhibitors for the Urokinase-Type Plasminogen Activator: Optimization of the P4 Position" J. Med. Chem. 2006, 49, 5785–5793.

(15) Boduszek, B.; Brown, A. D.; Powers, J. C. "alpha-Aminoalkylphosphonate di(chlorophenyl) esters as inhibitors of serine proteases" J. Enzyme Inhib. 1994, 8, 147–158.

(16) Mauricio, A. T. Heterocyclic alpha-aminoalkylphosphonate diphenyl esters as inhibitors of serine proteases : Part II: Basic alpha-aminoalkylphosphonate diphenyl esters as inhibitors of cathepsin G, Georgia Institute of Technology, 1996.

(17) Rarey, M.; Kramer, B.; Lengauer, T.; Klebe, G. " A fast flexible docking method using an incremental construction algorithm" J. Mol. Biol. 1996, 261, 470–489.

(18) Forli, S. Raccoon|AutoDock VS: an automated tool for preparing AutoDock virtual screenings http://autodock.scripps.edu/resources/raccoon (accessed Jul 8, 2014).

(19) Coombs, G. S.; Bergstrom, R. C.; Pellequer, J.-L.; Baker, S. I.; Navre, M.; Smith, M. M.; Tainer, J. A.; Madison, E. L.; Corey, D. R." Substrate specificity of prostate-specific antigen (PSA)" Chem. Biol. 1998, 5, 475–488.

(20) LeBeau, A. M.; Banerjee, S. R.; Pomper, M. G.; Mease, R. C.; Denmeade, S. R. " Optimization of peptide-based inhibitors of prostate-specific antigen (PSA) as targeted imaging agents for prostate cancer" Bioorg. Med. Chem. 2009, 17, 4888–4893.

(21) Denmeade, S. R.; Lou, W.; Lövgren, J.; Lovgren, J.; Maim, J.; Lilja, H.; Isaacs, J. T. " Specific and efficient peptide substrates for assaying the proteolytic activity of prostate-specific antigen" Cancer Res. 1997, 57, 4924–4930.

(22) Pronk, S.; Páll, S.; Schulz, R.; Larsson, P.; Bjelkmar, P.; Apostolov, R.; Shirts, M. R.; Smith, J. C.; Kasson, P. M.; van der Spoel, D.; Hess, B.; Lindahl, E. " GROMACS 4.5: a high-throughput and highly parallel open source molecular simulation toolkit" Bioinformatics 2013, 29, 845–854.

(23) Dahl, A. C. E.; Chavent, M.; Sansom, M. S. P. " Bendix: intuitive helix geometry analysis and abstraction" Bioinformatics 2012, 28, 2193–2194.

(24) Carugo, O.; Argos, P." Accessibility to internal cavities and ligand binding sites monitored by

protein crystallographic thermal factors" Proteins Struct. Funct. Bioinforma. 1998, 213, 201–213.

(25) Ménez, R.; Michel, S.; Muller, B. H.; Bossus, M.; Ducancel, F.; Jolivet-Reynaud, C.; Stura, E. " Crystal structure of a ternary complex between human prostate-specific antigen, its substrate acyl intermediate and an activating antibody" J. Mol. Biol. 2008, 376, 1021–1033.

How to cite this article:

Arben Kojtari, Jacob Babinec, Vishal Shah, Catherine Yang, and Hai-Feng Ji *Structure-Based Design Of Tripeptide Derivatives Of α -Aminoalkylphosphonate Esters For Prostate-Specific Antigen Inhibition* Br J Pharm Med Res , Vol.03, Issue 06, Pg.1478 - 1493, November - December 2018. ISSN:2456-9836 Cross Ref DOI : https://doi.org/10.24942/bjpmr.2018.390

Source of Support: Nil **Conflict of Interest:** None declared